Application Research of Data Processing Software in Experimental Teaching of Concrete Foundation

Chengqin Chen(✉), Wei Zhang, Hongjuan Wu, and Wanzhi Cao

School of Civil Engineering, Northwest Minzu University, Lanzhou, Gansu, China
346119862@qq.com

Abstract. Concrete materials have complexity, variability, and random uncertainty. How to help students better grasp the changing rules of concrete properties is a problem. It is necessary to combine a variety of data processing software for analysis. In this paper, the mechanical properties of concrete were the research object, using excel software for data processing and drawing. All students can quickly grasp and use it. We clarify the relation between stress and strain of concrete structure under load, and the constitutive connection of concrete is established. It is more consistent with a Bingham-type viscoplastic body. Furthermore, X-ray CT technology is used to scan the concrete section and analyze the failure mechanism of concrete, which accords with the Zaitsev-Wittmann aggregate interference model. Through rational use of data processing software, students are trained to use computer software to analyze experimental data, diagnose problems and solve problems, and improve students' practical ability and innovation abilities.

Keywords: Excel · Data processing · Concrete · The strength · bingham-like model

1 Introduction

The concrete foundation experiment is one of the compulsory introductory experiment courses for inorganic, nonmetallic materials engineering majors. It mainly studies the change rule of concrete material properties by practical methods. It is a very theoretical, helpful, and comprehensive course. Compared with other classes, concrete foundation experiment involves a large amount of experimental data, so the processing and analyzing the obtained data is an essential link to a physical chemistry experiment. The practice shows that although the students can complete the experimental operation, instrument use, and data acquisition, their ability to analyze the data could be more vital. Therefore, using data processing software to extract, process, and analyze experimental data is more than just convenient and accurate. But also can improve students' learning efficiency and comprehensive application ability of relevant knowledge [1]. It is helpful to cultivate students' ability to analyze and solve problems independently, and exercise students'

X. Yuan et al. (Eds.): ICEKIM 2023, AHCS 13, pp. 640–650, 2023.
https://doi.org/10.2991/978-94-6463-172-2_68

serious, rigorous and realistic experimental attitude [2, 3]. It lays a good data analysis foundation for a subsequent comprehensive experiment, undergraduate graduation project, and scientific research. Data processing is a vital link in the concrete foundation experiment course, but it is rarely discussed in the definite foundation experiment course and course teaching.

Concrete is a heterogeneous material consisting of solid particles, hardened cement mortar, micro-cracks, and micro-voids [4]. Significant differences exist in the mechanical properties of solid particles and mortar [5]. Therefore, the mechanical properties of concrete materials can not be correctly evaluated. And the composition is complex; the performance is variable, and the random uncertainty. Wittmann et al. [6] first proposed using the randomly distributed polygonal concrete aggregate model to study the meso-mechanical properties of concrete. Wang et al. [7]. Established a numerical concrete model containing pores based on elliptic and polygonal aggregate models and studied the influence of different aggregate shapes and porosity on the tensile strength of concrete. Deng Yongjun et al. [8]. Established a three-dimensional concrete mesoscopic geometric model. They study the influence of mesoscopic factors on a concrete ballistic deflection. Wu Cheng et al. [9]. Used the random aggregate model to study the effects of mortar, aggregate type, the volume fraction and established the penetration depth model of meso-concrete. Tian Wei et al. [10]. Reconstructed the three-dimensional pore structure of concrete based on CT scanning technology. Most of the research on concrete numerical simulation is to establish numerical concrete models corresponding to concrete samples through image comparison, and these models are very close to real concrete. Therefore, in the teaching practice content of this course, students are not only taught how to evaluate the performance of concrete from a macro perspective. But they also appropriately interspersed with the concrete numerical model based on the theory of damaged zones so that students can further understand the action mechanism of concrete.

2 Basic Overview of Concrete Strength Test

Concrete strength measurement is one of the important contents of the "Concrete Foundation Experiment Course" [11]. Ordinary Portland cement, sand, gravel, polycarboxylic acid water reducer, fine limestone powder, fly ash, and slag were selected as raw materials in the experiment. The limestone powder was added to concrete with different mixing methods and dosages for the same mix ratio. The microscopic structure analyzed various minerals in the concrete system and their hydration process. It explored the influence mechanism of limestone powder on the performance of concrete to provide theoretical and technical support for the production and application of SCC. Limestone powder dosage choices are 10%, 20%, and 30%. The slag content is fixed at 15%, and the content of fly ash is fixed at 20%. The volume of sand per cubic meter of concrete is the volume fraction of mortar. The design of the concrete mix ratio was calculated by "Technical Specifications for the Application of Self-compacting Concrete" (JGJ/T283–2012). The C30 concrete was selected for this test to study the limestone powder. The tangible mix ratio was shown in Table 1. Among them, the mass of water is 186.52 kg/m^3; the group of sand is 794.68 kg/m^3; the mass of stone is 863 kg/m^3; the mass of fly ash is 96 kg/m^3; the group of slag is 72 kg/m^3; the mass of water reducer is 2.39 kg/m^3.

Table 1. The Results of optimixation of proportion (kg/m^3)

No.	Cement	500mesh	400mesh	300mesh
NC	310.7	-	-	-
5L1	262.9	47.8	-	-
4L1	262.9	-	47.8	-
3L1	262.9	-	-	47.8
5L2	215.1	95.6	-	-
4L2	215.1	-	95.6	-
3L2	215.1	-	-	95.6
5L3	167.3	143.4	-	-
4L3	167.3	-	143.4	-
3L3	167.3	-	-	143.4
54L1	262.9	23.9	23.9	-
53L1	262.9	23.9	-	23.9
34L1	262.9	-	23.9	23.9
54L2	215.1	47.8	47.8	-
53L2	215.1	47.8	-	47.8
34L2	215.1	-	47.8	47.8
54L3	167.3	71.7	71.7	-
53L3	167.3	71.7	-	71.7
34L3	167.3	-	71.7	71.7
543L1	262.9	15.93	15.93	15.93
543L2	215.	31.87	31.87	31.87
543L3	167.3	47.8	47.8	47.8

Note:1.NC represents "No limestone powder added to concrete";1.L represents limestone powder, and 500 mesh, 400 mesh, and 325 mesh5,4,3 represent, respectively. The content of 10%, 20%, and 30% is represented by digital subscripts 1, 2, and 3. E.g:1L1 means that the single mixing fineness is 500 mesh limestone powder of 10%

3 To Excel Analysis of Concrete Strength Change Law

Concrete presents different changes when subjected to different load types. Students analyze its change rule. They commonly use data processing software, including Excel and Origin [12]. Excel software has a high penetration rate, is very easy to obtain, and the operation is simple and easy to master. But the functionality is relatively simple. For more complex data processing, it is necessary to assist with a large number of calculations, and there are many steps to draw a combination of multiple graphs. The efficiency is relatively low for the students. The Origin software is highly professional, convenient, and fast. The diagram drawn is beautiful and can accurately reflect the change law of

Table 2. The strength data for types of concrete in Excel

NO.	Compressive strength (MPa)		Flexural strength (MPa)		RFC (%)	
	3d	28d	3d	28d	3d	28d
NC	28.6	39.5	2.8	4.2	9.6	10.7
5L1	37.8	53.3	3.5	5.3	9.3	10.0
4L1	34.2	51.5	3.3	5.2	9.6	10.0
3L1	29.1	43.8	3.0	4.4	10.1	10.0
5L2	38.7	55.6	3.6	5.6	9.2	10.0
4L2	35.6	53.5	3.6	5.4	10.0	10.1
3L2	29.3	42.9	3.0	4.6	10.3	10.7
5L3	37.9	53.7	3.5	5.7	9.3	10.6
4L3	36.8	52.8	3.4	5.3	9.1	10.1
3L3	29.5	41.4	3.0	4.4	10.0	10.6
54L1	38.2	54.6	3.5	5.5	9.2	10.0
53L1	32.5	52.2	3.2	5.2	9.8	10.0
34L1	31.1	47.4	3.0	4.8	9.7	10.0
54L2	38.9	56.5	3.4	5.7	8.8	10.1
53L2	36.9	53.6	3.5	5.4	9.4	10.0
34L2	30.7	43.6	3.1	4.9	10.1	11.2
54L3	38.5	54.8	3.4	5.5	8.8	10.1
53L3	31.8	50.7	3.2	5.3	10.1	10.4
34L3	29.6	42.3	3.0	4.7	10.2	11.2
543L1	40.2	56.8	3.6	5.7	9.0	10.1
543L2	43.5	58.6	3.9	6.0	9.0	10.2
543L3	39.3	50.2	3.5	5.1	9.0	10.3

experimental data. But most of them are in English, which is difficult for some students to use. Most students learn the data processing method. This study takes the compressive and flexural properties of concrete as the research object. Excel data processing method was used to analyze the strength variation rule and optimize the concrete mix ratio. Input the test data into the excel worksheet, as shown in Table 2.

3.1 The Variation Law of Concrete Compressive Strength is Analyzed by Column Graph

Firstly, we select the first three columns of data in Table 2, select "Insert" → "chart" → "column chart", and then carry out coordinate layout, modify the coordinate axis, title, font and other information of horizontal and vertical coordinates, as shown in Fig. 1. The

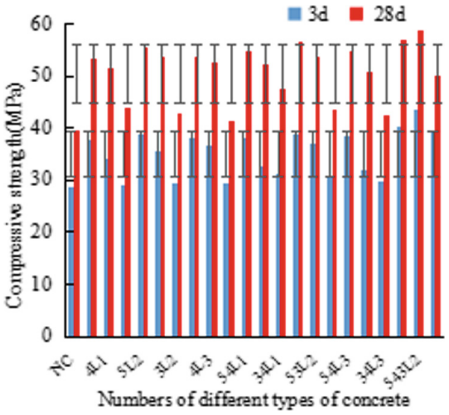

Fig. 1. Excel bar chart of concrete compressive strength

bar graph allows you to visually compare values across several categories. To further clarify the strength trend, you can choose "Chart Tool" → "Add Elements" → "Standard Deviation", which shows the shape "I" in the bar chart.

Figure 1 clearly shows the strength of concrete at different ages with different mixtures of limestone powder with different fineness [13]. According to Fig. 1, compared with the benchmark concrete, the 3d compressive strength of other 21 kinds of substantial increases by 32.17%, 19.58%, 1.75%, 35.31%, 24.48%, 2.45%, 32.52%, 28.67%, and 3.15%, respectively. 33.57%, 13.64%, 8.74%, 36.01%, 29.02%, 7.34%, 34.62%, 11.19%, 3.5%, 40.56%, 52.10%, 37.41%, 28d compressive strength increases 34.94%, 30.38%, 10.89%, 40.86%, 35.49%, 8.05%, 36.05%, 33.34%, 4.73%, 38.30%, 32.20%, 19.87%, 42.91%, 35.62%, 10.43%, 38.76%, respectively, 28.43%, 7.14%, 43.90%, 52.10% and27.01%. Under the condition of limestone powder content of 10%, compared with the benchmark concrete, the 3d and 28d compressive strengths of 543L1 were the highest, followed by 12L1 under different mixing methods. 3L1 was the lowest. Under the condition of limestone powder content of 20%, the 3d and 28d of 543L2 compressive strength under different mixing methods were the highest, followed by 12L2, and 3L2 is the lowest. Under the condition of limestone powder content of 30%, compared to the benchmark concrete, under different doping methods, 123L3 had the highest compressive strength, 12L3, and 3L3 had the lowest. Compared with NC, 543L2 has the largest deviation in the variation of compressive strength of 3d and 28d, followed by 543L1. This way-the data set's dispersion degree can reflect the concrete's early and late strength. That is the deviation degree of the data set relative to the mean of the data set.

3.2 The Flexural Strength of Concrete is Analyzed by Column Graph and Linear Fitting

We further study the influence of three kinds of limestone powder with different fineness on the bending strength of concrete under other mixing methods, the first column NC, 5L1, 5L2, and 5L3, as well as the bending strength values of 3d and 28d in the Excel

table are selected. Click "Insert" to choose "scatter diagram" and select the type "I." To clarify the influence of 500mesh limestone powder on the flex strength of concrete, like the graph, click "Chart Tool" and select the approach line in "Add Elements." According to the size of R^2, a reasonable linear fitting formula was selected and listed in Table 3. The appropriate modes of other single-doped 400mesh, single-doped 325mesh, double-doped, and triple-doped are the same as those in Figs. 2 (a), (b), (c), and (d).

As seen from Fig. 2 and Table 3, the limestone powder in different mixing methods, the flexural strength of concrete, and the amount of limestone powder were in the form of a quadratic parabola. R^2 represents the degree of similarity. When the R2 was more significant than 0.96, the flexural strength change of concrete at different dosages was consistent with $y = \alpha x^2 + \beta x + \gamma$.

Where: α was a negative value, indicating that the flexural strength of concrete was affected by the dosage, and there was an optimal dosage. When the limestone powder was less than the optimal dosage, the flexural strength of concrete increased with the dosage increased. That is, the more limestone powder dosage was added. However, when the dosage was higher than the optimum amount, the flexural strength of the concrete decreased. The size of βcould reflects the position of the optimal dosage. The larger the β, the higher the flexural strength, the higher the flexural strength, and the lower the vice versa. γ could reflect the minimum flexural strength. The γ value of concrete flexural strength of 3d was maintained between 1.5 and 2.5. And the γ value of flexural strength of 28d was maintained between 1.5 and 4.0.

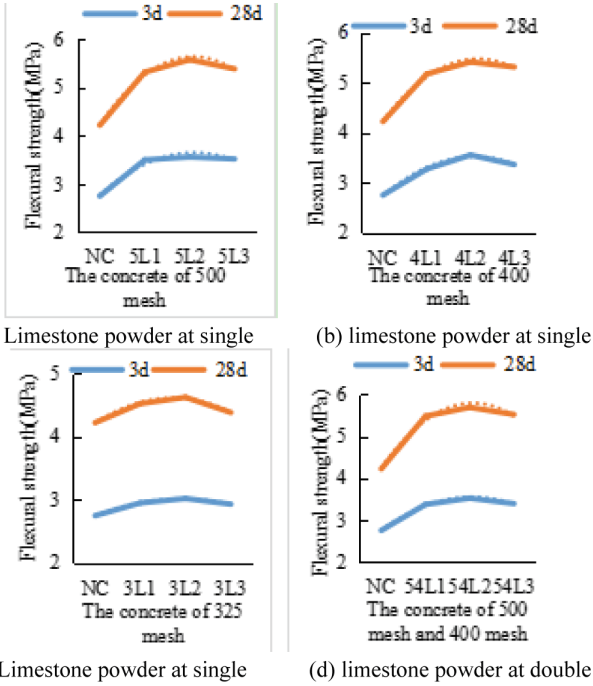

(a) Limestone powder at single (b) limestone powder at single

(c)Limestone powder at single (d) limestone powder at double

Fig. 2. Linear fitting graph of concrete flexural strength

Table 3. The strength data for types of concrete in Excel

No.		Equation.	α	β	γ	Maximum	R^2
(a)	3d	$y = -0.1975x^2 + 1.2245x + 1.7525$	-0.1975	1.2245	1.7525	3.10	0.96
	28d	$y = -0.3225x2 + 1.9895x + 2.5725$	-0.3225	1.9895	2.5725	3.08	0.99
(b)	3d	$y = -0.1775x^2 + 1.0985x + 1.8175$	-0.1775	1.0985	1.8175	3.09	0.99
	28d	$y = -0.2625x^2 + 1.6635x + 2.8375$	-0.2625	1.6635	2.8375	3.17	0.99
(c)	3d	$y = -0.0725x^2 + 0.4235x + 2.3975$	-0.0725	0.4235	2.3975	2.92	0.99
	28d	$y = -0.135x^2 + 0.733x + 3.615$	-0.135	0.733	3.615	2.71	0.99
(d)	3d	$y = -0.1875x^2 + 1.1445x + 1.8025$	-0.1875	1.1445	1.8025	3.05	0.99
	28d	$y = -0.3575x^2 + 2.1985x + 2.4125$	-0.3575	2.1985	2.4125	3.07	0.98

3.3 Concrete Damage Constitutive Model

The damaged concrete skin falls off, and the interior is the process of the slow formation and expansion of microcracks. From the macro point of view, it is mainly the interface crack caused by settlement and shrinkage between coarse aggregate and mortar. From the microscopic point of view, it is primarily the crack caused by uneven shrinkage in the mortar [14]. The damage model proposed by Loland and Mazars results from earlier research on the tensile mechanical behavior of concrete using damage [15]. According to the tensile stress-strain curve, the tensile curve is divided into two sections: before and after the stress peak. The damage expansion is divided into two areas, and the damage expansion in each room is simulated by different functions [16]. D rajcinovic derived the damage evolution equation with a method similar to that used in the study of plastic mechanics [17]. The creep damage model is because, under the action of high stress, the propagation of microcracks is an important cause of concrete creep and creep failure [18]. The nonlinear creep constitutive equation of elastic creep coupling damage is obtained by using the continuum damage mechanics method for the Response of concrete materials under different strain rates, both the stress peak and the strain value corresponding to the stress peak increase with the increase of strain rate [19]. The stress-strain curves of concrete under different uniaxial compression loads are shown in Fig. 3.

Seen from Fig. 3, concrete exhibits certain plasticity. Under long-term loading, concrete has obvious creep and viscoplastic damage constitutive relationship even at room temperature. The strain rate correlation and inelastic deformation characteristics of concrete are consistent with Bingham type viscoplastic body. The total strain rate consists

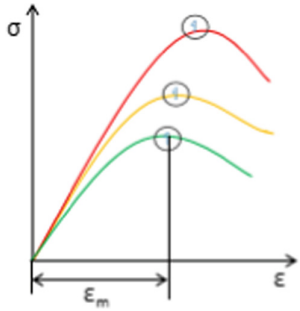

Fig. 3. The stress-strain curves of concrete

of two parts, namely the elastic strain rate and the viscoplastic strain rate:

$$\varepsilon = \varepsilon_e + \varepsilon_{vp} \tag{1}$$

Where, ε_e stands for elastic strain rate; ε_{vp} is the viscoplastic strain rate caused by stress.

$$\varepsilon_e = \frac{\sigma}{E} \tag{2}$$

$$\varepsilon_{vp} = \left(\frac{\sigma - \sigma_0}{\mu}\right)^n \tag{3}$$

E is the material's elastic modulus, σ_0 is the yield stress, μ is the viscosity coefficient, and n is the material constant.

The constitutive relation of concrete is established as follows without considering the damage:

$$\varepsilon = \varepsilon_e = \frac{\sigma}{E} (\sigma \leq \sigma_0) \tag{4}$$

$$\varepsilon = \varepsilon_e + \varepsilon_{vp} = \frac{\sigma}{E} + \left(\frac{\sigma - \sigma_0}{\mu}\right)^n (\sigma > \sigma_0) \tag{5}$$

3.4 Zaitsev-Wittmann Aggregate Interference Model

Concrete materials are easily affected by environmental factors, resulting in different cracks [20]. The Higgins-Bailey parallel microcrack model, Zaitsev-Wittmann aggregate interference model, and Wing Crack model are the main reasons for different concrete damage mechanisms. X-ray CT scanning technology was used to explore the internal structure of cement concrete, as shown in the figure. Therefore, to improve the cracking resistance of concrete, it is necessary to understand the cracking reason of concrete structure. Thus, when teaching this knowledge, the lecturer used X-ray CT images of concrete for analysis. In X-ray CT images, grayscale values are used for image processing. The grayscale value can reflect the density of the material. In the scanned cement

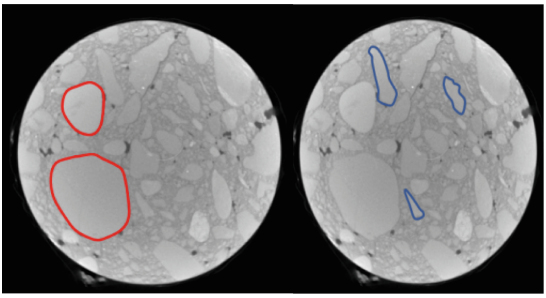

(a)Spherical aggregate (b)Needle flake aggregate

Fig. 4. X-ray CT image of concrete

concrete sections, as shown in Fig. 4, the parts with small grayscale value and dark color are cracks and no spaces, while the regions with considerable grayscale value and bright color are sand and cement.

The shape of aggregate particles determines the distance through which the energy dissipates along the aggregate profile. We have seen from Fig. 4 that for spherical aggregate, the length is shorter. In contrast, the distance passed by the wave along the aggregate profile for needle-flake entirety is much greater than the distance directly through the aggregate. Therefore, the energy dissipated by the impact elastic wave transmitted along the aggregate profile is greater than that of cutting and penetrating the aggregate, and the corner is the weak surface of the aggregate. So the microcracks will cut the aggregate along the edges and corners to form type II microcracks or directly through the aggregate to form type III microcracks. The spherical coarse aggregate has a blocking effect on the development of microcracks. This phenomenon is consistent with the Zaitsev-Wittmann aggregate interference model. Aggregate has a significant effect on crack propagation. After encountering aggregate, crack propagation spreads along the aggregate interface until cracking [21]. We have seen from Fig. 4 that for spherical aggregate, the length is shorter. In contrast, the distance passed by the wave along the aggregate profile for needle-flake entirety is much greater than the distance directly through the aggregate.

4 Conclusions

This paper uses Excel software to process and analyze the experimental data of concrete performance. Based on the compressive strength and flexural strength of concrete, it introduces in detail the processing process of a column chart, line chart, and accumulation area chart in Excel software and the analysis of experimental data. The column chart of concrete compressive strength shows that 543L2 has the most significant deviation, followed by 543L1, which can reflect the dispersion degree of the data set of early and late strength of concrete, namely, the deviation degree of the data set relative to the mean of the data set. The column diagram and linear fitting of concrete bending strength can be obtained as follows: the flexural strength change of concrete at different dosages was consistent with $y = \alpha x^2 + \beta x + \gamma$ if R^2 was more significant than 0.96. The accumulation area can be clearly analyzed in the diagram: the results of RFC at 3d and 28d

were between 8.5% and 11.2%. Under uniaxial compression, concrete exhibits certain plasticity. Under long-term loading, concrete also exhibits noticeable creep even. So the viscoplastic damage constitutive relationship is established. It conforms to the Bingham-type viscoplastic body. X-ray CT images of the concrete show that the internal structural damage of the concrete belongs to the Zaitsev-Wittmann aggregate interference model. We introduce the data processing software into the definite introductory experiment course; the data processing is convenient and fast, can improve the accuracy and precision of the experimental results, and ensure the scientific, objective, and intuitive results.

Acknowledgment. The research was funded by the Undergraduate Talent Training Quality Improvement Project at Northwest Minzu University, grant number 2022XJJG-70. This research was also funded by the "Gansu Province Education and Teaching Achievement Cultivation Project," grant number2020GSJXCGPY-02. This research was also funded by the "The second batch of new engineering research and practice projects of the Ministry of Education," grant number E-TMJZSLHY20202156.

References

1. Sun Bing, Wang Wenbin, Ma Yuchun. Teaching Application of Simulated Laboratory on Computer Monitoring System [J].Journal of Hainan Tropical Ocean University, 2015, 22(02):118–122.
2. Han Jianghong. Research on the application of project teaching method in Children's Clothing Design [J].Diet Science.,2017(18):131+133.
3. Chen Lintao, Lu Jianlong. Construction and Exploration of middle school physics experiment teaching mode under Man-machine collaboration [J]. Cultural and educational materials.2022(16):112–115.
4. Chen X M. Application of grey system theory to kinetic energy projectile penetration of concrete target [D]. China Academy of Engineering Physics,2012.
5. Shuai X L. Experimental study and finite element analysis of dynamic properties of concrete under impact load [D]. Hunan University,2013.
6. WITTMANN F H, ROELFSTRA P E, SADOUKI H. Simulation and analysis of composite structures [J]. Materials Science and Engineering. 1985 ,68(2):239- 248.
7. WANGXF, YANGZJ, YATESJR, et al. Monte Carlo simulations of mesoscale fracture modeling of concrete with random aggregates and pores [J]. Construction and Building Materials, 2015, 75:35–45.
8. DENG Yong-jun, CHEN Xiao-wei, YAO Yong.et al. On ballistie trjectory of rigid projectile normal penetration based on a meso scopic concrete [J]. Explosion and Shock W aves, 2017 ,37(3) :377–386.
9. WU Cheng, SHEN Xiao-jun, WANG Xiao-ming, et al. Numerical simulation on anti-penetration and penetration depth model of mesoscale concrete target [J]. Explosion and Shock Waves, 2018, 38 (6):1364- 1371.
10. TIAN Wei, ZHANG Peng-Kun, XIE Yong-li, et al. 3D distribution characteristics on concrete, porous structure under freeze-thaw env environment based on CT technique [J]. Journal of Chang a University: NaturalScience Edition.2016,36(3):4955.
11. Wang Yingfa, Xia Kun, Zhou Fengcai, et al. Application of rebound instrument to detect Concrete in Yellow Penetration Project [J]. Northeast Water Resources and Hydropower, 2015,33(04):65–67+70.

12. Guo Xiaopeng, Zhang Miaomiao, et al. Journal of Radiation Research and Technology, 2016,34(04):59-66.
13. Zhu K. Feasibility study on the application of limestone powder to replace part of cement in Ningxia commercial concrete [J]. Concrete and Cement Products,2017(05):93-95.
14. Wang K. Multi-scale analysis of concrete material and structure failure caused by meso-crack growth [D]. Southeast University,2015.
15. Yang S S. Analysis of dynamic response and continuous collapse of concrete frame structures under explosion [D]. Shandong University of Science and Technology,2012.
16. Xu P. Study on Static and Dynamic Mechanical Properties and Damage Mechanism of Steel Fiber Polymer Concrete Machine Tool Foundation [D]. Liaoning Technical University, 2006
17. Hu Peng. Dynamic Response and continuous collapse analysis of frame structures under explosion impact load [D]. Chang ‘an University,2008
18. Feng Chen. Analysis of Stress-Strain Field at V-Notch Tip of Concrete Material [D]. Harbin Engineering University,2008
19. Yu Qi. Experimental Study on SHPB Impact Resistance of Plain Concrete under High Temperature [D]. Hunan University,2011.
20. Lin Jiantai. Crack Problem of Concrete Structure and its Prevention Countermeasures [J]. Sichuan Building Materials,2018,44(09):86-87.
21. Xue Mingchen. Failure Analysis of Concrete and Its Strengthening and Toughening Materials [D]. Shandong University of Technology,2006.